OPEN

Citation: Oncogenesis (2013) **2**, e74; doi:10.1038/oncsis.2013.38

www.nature.com/oncsis

SHORT COMMUNICATION

Expression of *PIK3CA* mutant E545K in the mammary gland induces heterogeneous tumors but is less potent than mutant H1047R

DS Meyer[1,4,5], S Koren[1,4], C Leroy[1,2], H Brinkhaus[1], U Müller[1], I Klebba[1,6], M Müller[2], RD Cardiff[3] and M Bentires-Alj[1]

The phosphoinositide 3-kinase (PI3K) signaling cascade is a key mediator of cellular growth, survival and metabolism and is frequently subverted in human cancer. The gene encoding for the alpha catalytic subunit of PI3K (*PIK3CA*) is mutated and/or amplified in ~30% of breast cancers. Mutations in either the kinase domain (H1047R) or the helical domain (E545K) are most common and result in a constitutively active enzyme with oncogenic capacity. *PIK3CA*^{H1047R} was previously demonstrated to induce tumors in transgenic mouse models; however, it was not known whether overexpression of *PIK3CA*^{E545K} is sufficient to induce mammary tumors and whether tumor initiation by these two types of mutants differs. Here, we demonstrate that expression of *PIK3CA*^{E545K} in the mouse mammary gland induces heterogenous mammary carcinomas but with a longer latency than *PIK3CA*^{H1047R}-expressing mice. Our results suggest that the helical domain mutant *PIK3CA*^{E545K} is a less potent inducer of mammary tumors due to less efficient activation of downstream Akt signaling.

Oncogenesis (2013) **2,** e74; doi:10.1038/oncsis.2013.38; published online 30 September 2013

Subject Categories: Cellular oncogenes

Keywords: PIK3CA; PI3K; breast cancer

INTRODUCTION

The phosphoinositide 3-kinase (PI3K) pathway is a key regulator of cell growth, proliferation, metabolism and survival and is often found to be hyperactivated in human cancer.[1,2] The most common aberrations of the PI3K pathway include mutation and/or amplification of *PIK3CA*,[3–7] the gene encoding the alpha catalytic subunit of the kinase (p110α), loss of expression of the PTEN phosphatase that reverses PI3K action, activation downstream of oncogenic receptor tyrosine kinases and mutation/amplification of Akt.[1] Hyperactivation of the PI3K pathway increases tumorigenicity by reducing cell death and increasing cell proliferation, migration, invasion, metabolism and angiogenesis.[1,2] It also enhances resistance to chemotherapy.[8]

The majority of mutations in *PIK3CA* occur at two 'hotspots' within the kinase (H1047R) and helical domains (E542K and E545K) of p110α.[6,9] These mutations lead to a constitutively active enzyme, transform cells *in vitro*, and enhance tumorigenicity in xenograft models.[10–13] Notably, different mechanisms underlie the gain-of-function activities of helical- and kinase domain mutants. While *PIK3CA*^{E545K} is independent of binding to the adaptor molecule p85 but requires interaction with Ras-GTP, the *PIK3CA*^{H1047R} mutant is highly dependent on p85 for its oncogenic capacity but independent of Ras-GTP.[14]

PIK3CA gain-of-function mutations are found in ~30% of human breast cancers[3,6,15–17] and most likely occur at an early stage of breast carcinoma development, as suggested by the similar mutation frequencies in *PIK3CA* found in pure ductal carcinoma *in situ*, ductal carcinoma *in situ* adjacent to invasive ductal carcinoma, and invasive ductal carcinoma.[18] Evaluation of the clinical outcome of genomic alterations in *PIK3CA* has produced contradictory results.[15,19,20] However, these studies showed that alterations in different exons of *PIK3CA* have varying impacts on tumor development and progression and, therefore, differ in prognostic value. For example, both mutations are associated with lower grade and hormone receptor-positive tumors, but *PIK3CA*^{H1047R} mutants are strongly associated with lymph-node negativity and *PIK3CA*^{E545K} mutants with older age at diagnosis, indicating the different oncogenic potentials of the H1047R and E545K mutations.[19] This is further supported by the different frequencies of E545K (~6%) and H1047R (~15%) mutations in breast cancer.[17,21] *In vivo* transplantation assays have demonstrated *PIK3CA*^{H1047R} to be more potent in inducing tumors[10] but another study found no trend,[12] and the exact impact of these mutations on breast cancer has remained controversial.

We and others have reported that expression of *PIK3CA*^{H1047R} in the mammary gland induces heterogeneous tumors.[22–25] To determine which *PIK3CA* mutant shows higher oncogenic activity *in vivo*, we generated a novel conditional mouse model expressing *PIK3CA*^{E545K}. We have demonstrated that *PIK3CA*^{E545K} induces heterogeneous mammary tumors that express basal and luminal markers but is a less potent oncogene *in vivo* than *PIK3CA*^{H1047R}.

[1]Mechanisms of Cancer, Friedrich Miescher Institute for Biomedical Research, Basel, Switzerland; [2]Developmental and Molecular Pathways, Novartis Institutes for Biomedical Research, Basel, Switzerland and [3]Department of Pathology, Center for Comparative Medicine, University of California Davis, Davis, CA, USA. Correspondence: Dr M Bentires-Alj, Mechanisms of Cancer, Friedrich Miescher Institute for Biomedical Research, Maulbeerstrasse 66, 4058, Basel, Switzerland.
E-mail: bentires@fmi.ch
[4]These authors contributed equally to this work.
[5]Current address: Helen Diller Family Comprehensive Cancer Center, School of Medicine, University of California San Francisco (UCSF), San Francisco, CA, USA.
[6]Current address: Department of Biosystems Science and Engineering (D-BSSE), ETH Zürich, Basel, Switzerland.
Received 17 June 2013; revised 13 August 2013; accepted 20 August 2013

RESULTS AND DISCUSSION

Expression of *PIK3CA*^{E545K} but not wild-type *PIK3CA* induces mammary tumors

We and others have shown that *PIK3CA*^{H1047R} induces mouse mammary carcinomas.[22–25] To test whether overexpression of wild-type human *PIK3CA* (*PIK3CA*^{wt}) or *PIK3CA*^{E545K} also induces mammary tumors, we generated novel transgenic mice that conditionally express *PIK3CA*^{wt} or *PIK3CA*^{E545K} (Figure 1a). To achieve equivalent transgene expression, we integrated *PIK3CA*^{wt} or *PIK3CA*^{E545K} into the ROSA26 locus using recombinase-mediated cassette exchange.[26] Correct integration of the target cassettes was confirmed in the resulting *PIK3CA*^{wt} and *PIK3CA*^{E545K} lines (Figure 1b, left). *PIK3CA*^{wt} and *PIK3CA*^{E545K} animals were then crossed to WAPiCre mice in which expression of recombinase Cre is controlled by the whey acidic protein (WAP) promoter, which is mainly active in secretory mammary epithelial cells, and expression of the transgenes confirmed (Figure 1b, *right*).[27–30] This enabled us to directly compare the kinetics of tumor onset in *PIK3CA*^{wt} and *PIK3CA*^{E545K} mice, and the previously reported WAPiCre *PIK3CA*^{H1047R} mice.[22]

The resulting bi-transgenic WAPiCre *PIK3CA*^{wt} and WAPiCre *PIK3CA*^{E545K} female mice were impregnated to achieve maximal Cre-mediated recombination and the pups removed 1 day after delivery. All WAPiCre *PIK3CA*^{E545K} mice developed mammary tumors on average 80 (±10) days after delivery, whereas parous WAPiCre *PIK3CA*^{wt} mice did not form tumors within 520 days (Figure 1c). This indicates that overexpression of wild-type *PIK3CA* itself is insufficient to induce mammary tumors. Of note, the latency to tumor onset in WAPiCre *PIK3CA*^{E545K} animals was significantly longer than that observed previously for WAPiCre *PIK3CA*^{H1047R} mice (36 (±4.9) days).[22] We also crossed *PIK3CA*^{E545K} and *PIK3CA*^{H1047R} lines to CAGs-CreERT2 mice that express a tamoxifen-inducible Cre/estrogen receptor (ER) fusion protein under the control of a modified β-actin promoter; this results in the expression of Cre-ER in virtually all cells. Unexpectedly, bi-transgenic CAGs-Cre *PIK3CA*^{E545K} and *PIK3CA*^{H1047R} mice died by the age of 4 months even when no tamoxifen was administered. Although we were unable to identify the exact cause of death, we concluded that leakiness of the CAGs-CreERT2 system caused premature and deleterious *PIK3CA*^{E545K} or *PIK3CA*^{H1047R} expression in various tissues of these mice (DSM and MB-A, unpublished observations).

To compare the tumor-initiating potential of the two different *PIK3CA* mutants, we then transplanted pieces of mammary gland tissue from CAGs-CreERT2 *PIK3CA*^{E545K} or *PIK3CA*^{H1047R} donor mice previously treated with tamoxifen into cleared fat pads of Balb/c mice. The mammary glands reconstituted by either CAGs-CreERT2 *PIK3CA*^{E545K} or *PIK3CA*^{H1047R}-derived epithelium were hyperplastic (data not shown) and eventually formed tumors after 229 (±17, *PIK3CA*^{H1047R}) and 336 days (±20, *PIK3CA*^{E545K}), respectively (Figure 1d). As observed in the WAPiCre mouse cohorts, *PIK3CA*^{E545K} was significantly less potent than *PIK3CA*^{H1047R} in the induction of mammary carcinomas, which is a possible explanation for the lower frequency of E542K/E545K mutations in human breast cancer.[17,21]

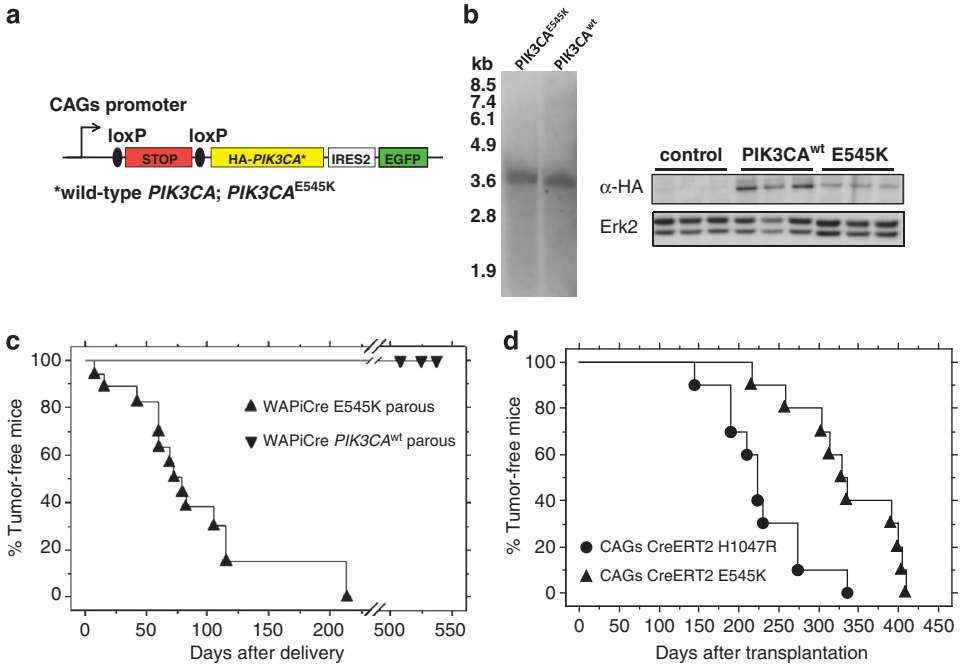

Figure 1. Overexpression of *PIK3CA* mutant *PIK3CA*^{E545K} but not *PIK3CA*^{wt} induces mammary tumors. (**a**) Schematic of the constructs used for generating transgenic mice conditionally expressing human wild-type and mutant 5′-terminally HA-tagged *PIK3CA*. Vectors were constructed in which the *PIK3CA* cDNA is flanked by a floxed STOP cassette upstream and an *IRES2-EGFP* reporter element downstream. The transgene is driven by a modified chicken β-actin (CAGs) promoter. The vector was introduced into a modified Rosa26 locus of Balb/c mouse embryonic stem cells by recombinase-mediated cassette exchange. (**b**) Southern blot of genomic DNA from *PIK3CA*^{E545K} and *PIK3CA*^{wt} transgenic mice (*left*) and immunoblots of lysates from mammary glands isolated 12 h after onset of involution from WAPiCre control, WAPiCre *PIK3CA*^{wt} and WAPiCre *PIK3CA*^{E545K} mice (each $n=3$) probed for HA. Erk2 levels were used as a control for equal loading (*right*). (**c**) Kaplan–Meier plot showing tumor onset in parous WAPiCre *PIK3CA*^{wt} ($n=8$) and WAPiCre E545K ($n=16$) mice. The mice were impregnated and the pups weaned 1 day after delivery. WAPiCre *PIK3CA*^{wt} mice did not develop palpable tumors within 520 days whereas mice expressing *PIK3CA*^{E545K} developed tumors on average 80 (±10) days after delivery. (**d**) Seven-week-old CAGs-CreERT2 *PIK3CA*^{E545K} and *PIK3CA*^{H1047R} donor mice were treated with tamoxifen on 3 consecutive days for transgene induction and fragments of glands were transplanted into cleared fat pads of three-week-old Balb/c recipient mice. Kaplan–Meier curves show tumor onset in recipient Balb/c mice transplanted with CAGs-CreERT2 *PIK3CA*^{E545K}- ($n=10$) or CAGS-CreERT2 *PIK3CA*^{H1047R}-derived mammary glands ($n=10$). Balb/c mice developed palpable tumors on average 336 (±20) days (*PIK3CA*^{E545K}) or 229 (±17) days (*PIK3CA*^{H1047R}) after transplantation; $P=0.0033$.

WAPiCre *PIK3CA*^{E545K}-evoked mammary tumors are heterogeneous

Examination of 30 WAPiCre *PIK3CA*^{E545K}-derived tumors identified 6 distinct histotypes. By far the most prevalent tumor phenotype was adenosquamous carcinoma (60%) (Figures 2a and b), which was also the most common histotype formed by WAPiCre *PIK3CA*^{H1047R} mice (54.6%).[22] Adenocarcinomas (23.3%) and carcinomas (6.7%) were also observed albeit at lower frequencies (Figures 2a and b). An adenocarcinoma with squamous metaplasia (3.3%), an adenomyoepithelioma (3.3%) and spindle cell tumor (3.3%) were observed in one tumor only (Figures 2a and b). The low frequency of adenomyoepithelioma in WAPiCre *PIK3CA*^{E545K} mice is in stark contrast to the WAPiCre *PIK3CA*^{H1047R} animals, in which adenomyoepitheliomas accounted for ~23% of the tumors.[22] A further discrepancy between mice expressing *PIK3CA*^{E545K} or *PIK3CA*^{H1047R} was the complete absence of diffuse and invasive adenocarcinomatosis in WAPiCre *PIK3CA*^{E545K}-derived glands, a histological feature that was displayed by all tumor-surrounding tissue in WAPiCre *PIK3CA*^{H1047R} mice.[22]

The *PIK3CA*^{E545K}-induced tumors were stained for luminal cytokeratin 18 (K18), basal/myoepithelial cytokeratin 14 (K14), and myoepithelial α-smooth muscle actin (α-SMA) markers. The most frequent histotypes, adenosquamous carcinoma and adenocarcinoma, were positive for both luminal K18 and basal K14 (Figure 2c). In tumors of the adenosquamous carcinoma type, the relative tumor areas positive for K18 and K14 were ~35% and ~39%, respectively (Figure 2d) and largely negative for α-SMA (<1%) (Figure 2d). WAPiCre *PIK3CA*^{E545K}-evoked adenosquamous carcinomas also stained positive for ER (~8% of the tumor cells) and displayed a high proportion of Ki-67-positive cells (~35%) (Figures 2c and d). The relative tumor areas and cells positive for K14, K18, α-SMA, ER and Ki-67 were very similar to those observed in *PIK3CA*^{H1047R}-driven adenosquamous carcinomas.[22] However, the number of apoptotic cells staining positively for cleaved

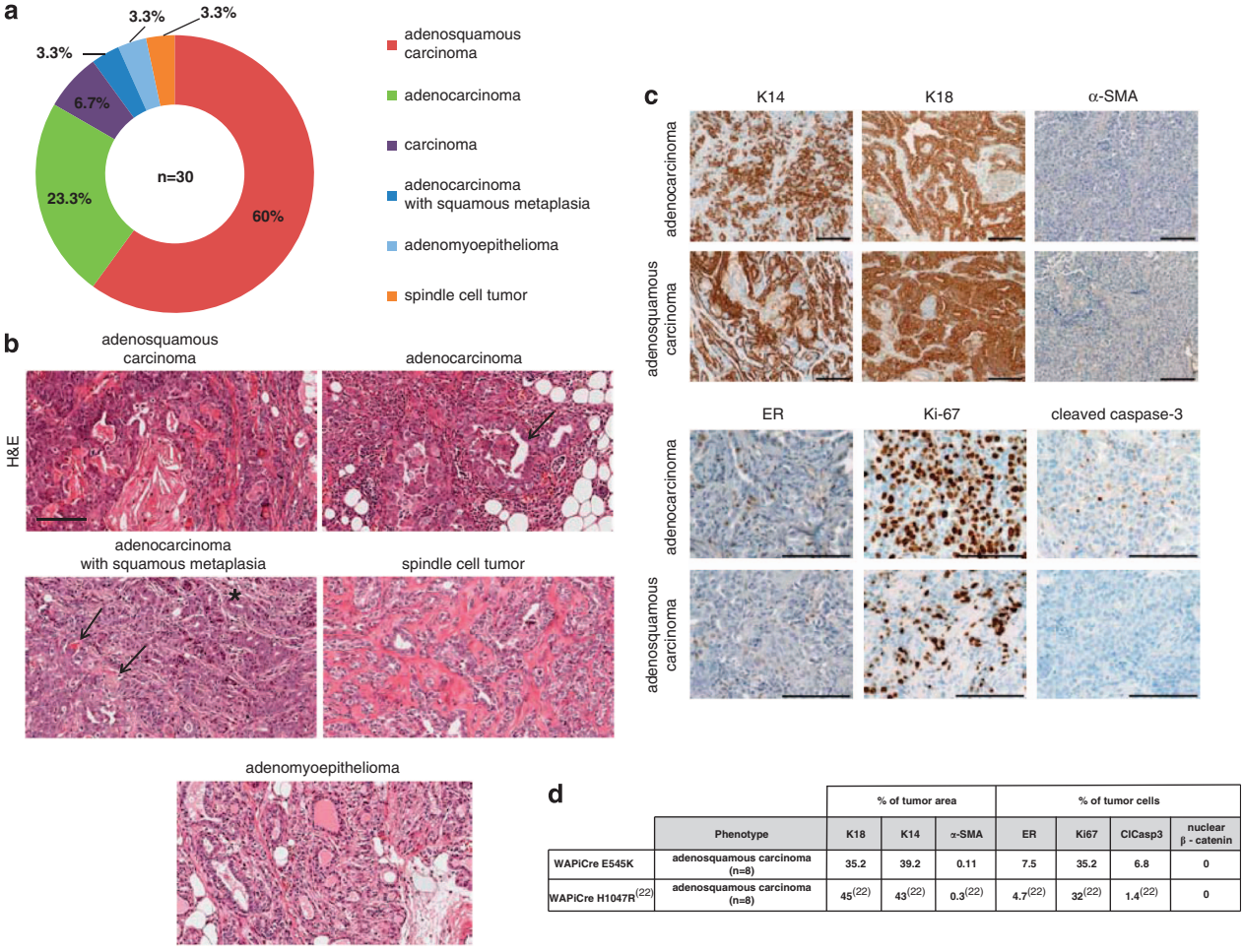

d

		% of tumor area			% of tumor cells			
	Phenotype	K18	K14	α-SMA	ER	Ki67	ClCasp3	nuclear β - catenin
WAPiCre E545K	adenosquamous carcinoma (n=8)	35.2	39.2	0.11	7.5	35.2	6.8	0
WAPiCre H1047R[22]	adenosquamous carcinoma (n=8)	45[22]	43[22]	0.3[22]	4.7[22]	32[22]	1.4[22]	0

Figure 2. WAPiCre *PIK3CA*^{E545K}-evoked tumors are heterogeneous and express basal and luminal cytokeratins. (**a**) Diagram showing relative abundance of adenosquamous carcinoma (60%, *red*), adenocarcinoma (23.3%, *green*), carcinoma (6.7%, *purple*), adenocarcinoma with squamous metaplasia (3.3%, *dark blue*), adenomyoepithelioma (3.3%, *light blue*) and spindle cell tumor (3.3%, *orange*) among tumors ($n = 30$) from parous WAPiCre *PIK3CA*^{E545K} mice. (**b**) H&E-stained tumor sections of the indicated histotypes from parous WAPiCre *PIK3CA*^{E545K} mice. The top-left image shows a representative adenosquamous carcinoma with glands and squamous features. The top-right image shows an adenocarcinoma; the arrows indicate the gland lumen. The glands are lined by malignant epithelium. The center-left image shows an adenocarcinoma with squamous metaplasia; the asterisk shows an area with glands and the arrow indicates areas of metaplasia. The center-right image shows a spindle cell tumor with possible osseous metaplasia, intense pink stroma and large cells in the interstices. The bottom image shows an adenomyoepithelioma. Scale bar = 100 μm. (**c**) Immunostaining for K14, K18, α-SMA, ER, Ki67 and cleaved caspase-3. Scale bars = 50 μm. (**d**) Quantification of immunostaining for K18, K14, α-SMA, ER, Ki67 and cleaved caspase-3 isolated from parous WAPiCre *PIK3CA*^{E545K}-evoked adenosquamous carcinomas ($n = 8$). The data are presented as percentages of positive tumor area and tumor cells. Histological features of WAPiCre *PIK3CA*^{E545K}-evoked adenosquamous carcinomas are compared with those of WAPiCre *PIK3CA*^{H1047R}-evoked adenosquamous carcinomas previously reported.[22]

caspase-3 was higher in *PIK3CA* $PIK3CA^{E545K}$-evoked adenosquamous carcinomas (~7%) (Figures 2c and d) than those derived from WAPiCre H1047R mice (~1%),[22] indicating that $PIK3CA^{H1047R}$ is a more potent suppressor of apoptosis than $PIK3CA^{E545K}$ in mammary tumors.

In summary, both $PIK3CA^{E545K}$ and $PIK3CA^{H1047R}$ produced K14/K18-positive tumors of various histotypes, with the adenosquamous carcinoma type being the most common in both transgenic models. However, differences between the mouse models included low abundance of adenomyoepitheliomas and the absence of adenocarcinomatosis in WAPiCre $PIK3CA^{E545K}$ mice.

The variations in tumor histotypes and the discrepancy in tumor latency in WAPiCre $PIK3CA^{E545K}$ and $PIK3CA^{H1047R}$ mice suggest that different mechanisms underlie tumor initiation by these mutants. To gain a mechanistic insight that might explain these differences, we investigated whether pregnancy accelerates tumor onset in WAPiCre $PIK3CA^{E545K}$ as it does in WAPiCre $PIK3CA^{H1047R}$ mice.[22] Pregnancy accelerated tumor onset in WAPiCre $PIK3CA^{E545K}$ mice, reducing latency from 228 ± 15 days in nulliparous to 165 ± 10 days in parous mice (Figure 3a). Interestingly, pregnancy appeared to accentuate the difference in tumor latency between WAPiCre $PIK3CA^{E545K}$ and $PIK3CA^{H1047R}$ mice, shown by 32 days difference in nulliparous vs 48 days difference in parous mice (Figure 3a).[22] We showed previously that a pregnancy-induced delay in mammary gland involution accounts, at least in part, for accelerated tumor kinetics in parous vs nulliparous $PIK3CA^{H1047R}$ mice.[22] Thus, we hypothesized here that the longer tumor latency of parous WAPiCre $PIK3CA^{E545K}$ compared with parous WAPiCre $PIK3CA^{H1047R}$ animals is the result of a less-pronounced involution delay. Comparison of WAPiCre $PIK3CA^{E545K}$ and WAPiCre $PIK3CA^{H1047R}$ glands 15 days after weaning revealed a dramatic delay in involution compared with control animals (Figure 3b). The relative gland area occupied by epithelial cells was the same in WAPiCre $PIK3CA^{E545K}$ and $PIK3CA^{H1047R}$ mice and significantly larger than in WAPiCre control glands (Figure 3c). Similarly, there was no difference in the number of apoptotic or proliferating cells in glands expressing either of the *PIK3CA* mutations (Figure 3d). Interestingly, glands from WAPiCre $PIK3CA^{wt}$ mice, which did not form tumors, displayed normal involution and numbers of apoptotic and proliferating cells similar to the controls (Figure 3), indicating that the delay in involution is caused by mutant *PIK3CA* rather than by

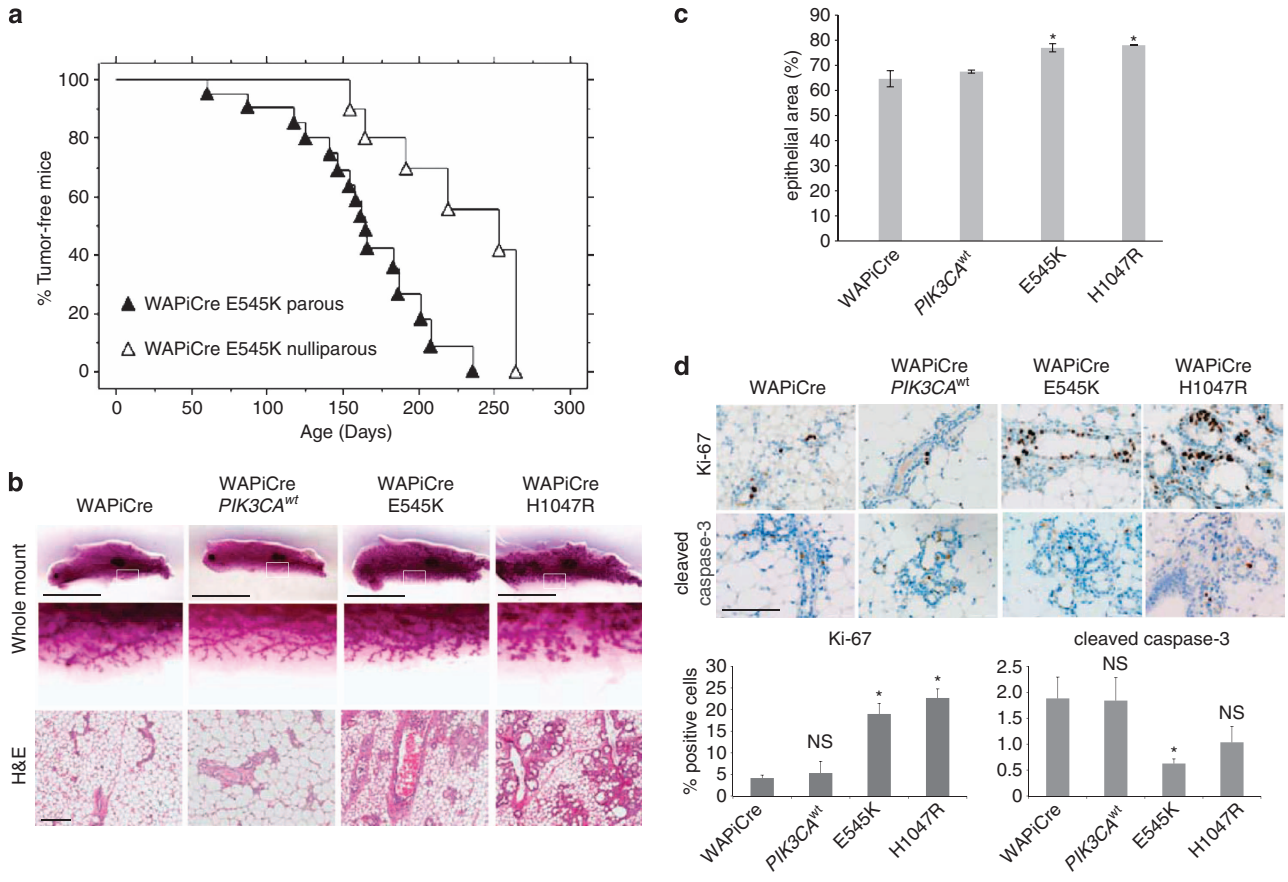

Figure 3. Pregnancy accelerates *PIK3CA*-evoked tumorigenesis and *PIK3CA* mutants delay mammary gland involution. (**a**) Kaplan–Meier curves showing tumor onset in parous WAPiCre $PIK3CA^{E545K}$ ($n = 16$) and nulliparous WAPiCre $PIK3CA^{E545K}$ ($n = 6$) animals. Parous WAPiCre $PIK3CA^{E545K}$ mice developed palpable tumors on average after 165 (± 10) days whereas nulliparous mice developed tumors on average after 228 (± 15) days ($PIK3CA^{E545K}$); $P = 0.0023$. (**b**) Representative images of whole mount (*top panels*), magnification of whole mount (*center panels*) and H&E (*lower panels*) staining of involuting glands from WAPiCre control, WAPiCre $PIK3CA^{wt}$, WAPiCre $PIK3CA^{E545K}$ and WAPiCre $PIK3CA^{H1047R}$ mice as indicated. The glands were isolated 15 days after removal of the pups. Scale bar = 1 cm (whole mounts). Scale bar = 100 μm (H&E sections). (**c**) Bar graph showing relative epithelium to total gland area of involution at day 15 in whole mounts prepared from WAPiCre control ($n = 3$), WAPiCre $PIK3CA^{wt}$ ($n = 4$), WAPiCre $PIK3CA^{E545K}$ ($n = 4$) and WAPiCre $PIK3CA^{H1047R}$ ($n = 2$). Means ± s.d. are shown; $P = 0.001$ (WAPiCre vs WAPiCre $PIK3CA^{E545K}$); $P = 0.01$ (WAPiCre vs WAPiCre $PIK3CA^{H1047R}$); $P = 0.46$ (WAPiCre $PIK3CA^{E545K}$ vs WAPiCre $PIK3CA^{H1047R}$). (**d**) Immunostaining for Ki67 and cleaved caspase-3 of day 15 involuting glands from WAPiCre control, WAPiCre $PIK3CA^{E545K}$ and WAPiCre^{H1047R} mice (*upper panels*). Scale bar = 50 μm. Quantification of Ki67- and cleaved caspase-3-positive cells (*lower panels*). Means ± s.e.m. are shown. *For Ki67-positive cells: $P = 2.18 \times 10^{-5}$ (WAPiCre vs WAPiCre $PIK3CA^{E545K}$), $P = 2.90 \times 10^{-7}$ (WAPiCre vs WAPiCre $PIK3CA^{H1047R}$). For cleaved caspase-3-positive cells: $P = 6.55 \times 10^{-3}$ (WAPiCre vs WAPiCre $PIK3CA^{E545K}$). NS = not significant.

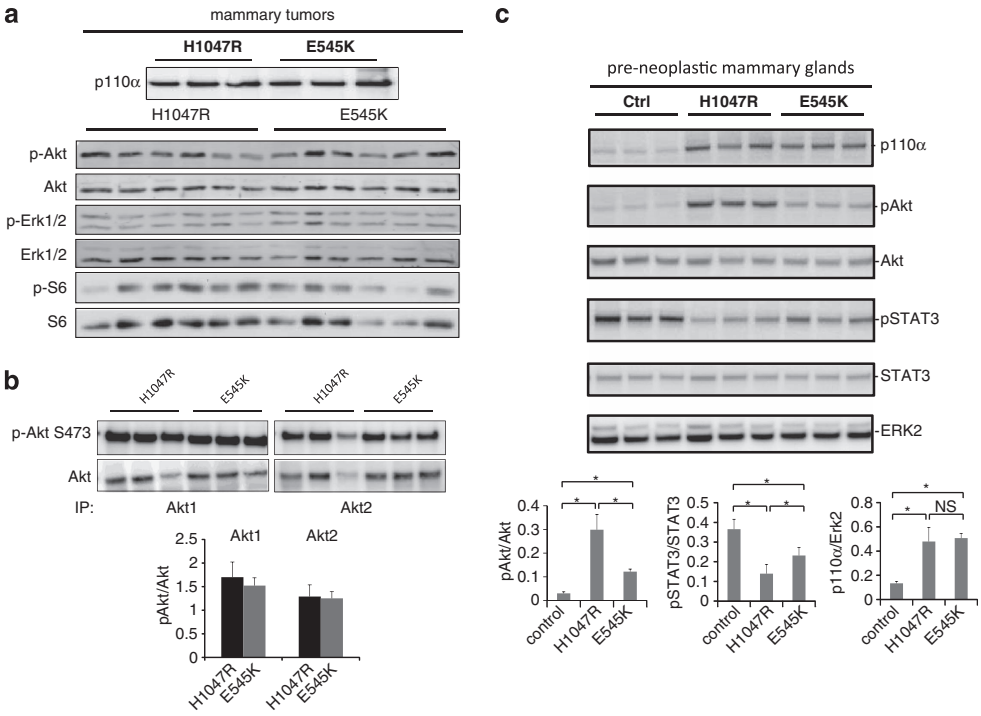

Figure 4. WAPiCre *PIK3CA*^{E545K} involuting glands show reduced pAkt and increased pSTAT3 compared with WAPiCre *PIK3CA*^{H1047R} at 12 h of involution. (**a**) Immunoblots of lysates from WAPiCre *PIK3CA*^{E545K} and WAPiCre *PIK3CA*^{H1047R} mammary tumors probed for the indicated proteins. (**b**) Lysates of mammary tumors from WAPiCre *PIK3CA*^{E545K} and WAPiCre *PIK3CA*^{H1047R} mice were first immunoprecipitated with antibodies against either Akt1 or Akt2 and then probed for total Akt or S473 pAkt (*upper panels*). Bar graph showing relative levels of S473 pAkt normalized to total Akt in Akt1 or Akt2 immunoprecipitates (*lower panel*). (**c**) Lysates of mammary glands isolated 12 h after onset of involution from WAPiCre control, WAPiCre *PIK3CA*^{H1047R} and WAPiCre *PIK3CA*^{E545K} mice (each $n = 3$) probed for p110α, pAkt, Akt, pSTAT3, STAT3 and ERK2 as a loading control (*upper panels*). Bar graphs showing relative amounts of pAkt (normalized to total Akt), pSTAT3 (normalized to total STAT3) and p110α (normalized to ERK2) in lysates of WAPiCre control, WAPiCre *PIK3CA*^{H1047R} and WAPiCre *PIK3CA*^{E545K} mammary glands (*lower panels*). *WAPiCre vs WAPiCre *PIK3CA*^{H1047R}: For pAkt $P = 3.8 \times 10^{-5}$; for pSTAT3 $P = 0.002$; for p110α $P = 0.007$. WAPiCre vs WAPiCre *PIK3CA*^{E545K}: For pAkt $P = 1.8 \times 10^{-4}$; for pSTAT3 $P = 0.02$; for p110α $P = 8.8 \times 10^{-5}$. WAPiCre *PIK3CA*^{H1047R} vs WAPiCre *PIK3CA*^{E545K}: for pAkt $P = 2.5 \times 10^{-4}$; for pSTAT3 $P = 0.047$; for p110α $P = 0.7$. NS = not significant.

overexpression of the transgene. In summary, *PIK3CA*^{E545K} and *PIK3CA*^{H1047R} transgene expression caused a dramatic but comparable delay in involution and, therefore, involution does not explain the different tumor kinetics observed in parous vs nulliparous mice expressing these mutations.

Comparison of lysates from WAPiCre *PIK3CA*^{E545K}- and WAPiCre *PIK3CA*^{H1047R}-derived mammary glands and tumors showed equal expression of p110α in tumors from both transgenic models (Figure 4a). Despite the enhanced oncogenic potential of the PIK3CA^{H1047R} mutant, no differences in activation of the PI3K/Akt or the Erk pathways were observed in the tumors (Figure 4a). Similarly, a more detailed analysis of Akt1 and Akt2 isoform-specific phosphorylation revealed no difference between *PIK3CA*^{E545K}- and WAPiCre *PIK3CA*^{H1047R}-induced signaling (Figure 4b). Conceivably, by the time mammary tumors were established, numerous secondary mutations had resulted in a tumor heterogeneity that compromises the detection of potentially subtle differences in oncogenic signaling induced by either *PIK3CA* mutant. To circumvent this, we investigated molecular signaling events in mutant *PIK3CA*-expressing epithelial cells at an early pre-neoplastic stage. Protein lysates from mammary glands isolated 12 h after the onset of involution revealed increased activation of Akt and decreased phosphorylation of the signal transducer and activator of transcription (STAT) 3 in mutant relative to control glands. Notably, both hyperactivation of Akt and hypoactivation of STAT3 were more pronounced in *PIK3CA*^{H1047R} than in *PIK3CA*^{E545K} glands (for pAkt $P = 2.5 \times 10^{-4}$; for pSTAT3 $P = 0.047$) (Figure 4c).

In summary, we found that overexpression of *PIK3CA*^{E545K} in a transgenic mouse model potently induces heterogeneous mammary tumors whereas overexpression of wild-type *PIK3CA* does not. Notably, although *PIK3CA*^{E545K} evokes tumors with 100% penetrance it is a weaker inducer of mammary tumors than *PIK3CA*^{H1047R} in two independent mouse models in which mutant *PIK3CA* is either driven by the WAP or by the CAGs promoter. This may explain the lower frequency of helical vs kinase domain mutations in human breast cancer.[13] We found differences in Akt and STAT3 activation in pre-neoplastic mammary glands from *PIK3CA*^{E545K} and *PIK3CA*^{H1047R} transgenic mice that may explain the longer tumor latency observed in WAPiCre *PIK3CA*^{E545K} compared with WAPiCre *PIK3CA*^{H1047R} mice.

The novel transgenic mouse models reported here provide excellent tools to further dissect the activities of different *PIK3CA* mutants in tumor initiation *in vivo* and to investigate drug responses to the ever-increasing number of PI3K pathway inhibitors.

MATERIALS AND METHODS

Transgenic mice

We constructed a vector with a transcriptional STOP sequence flanked by *loxP* sites upstream of the 5′-terminally HA-tagged human *PIK3CA* cDNA (Addgene, Cambridge, MA, USA) and an *IRES2-EGFP* reporter element (pIRES2-EGFP vector; Clontech, Mountain View, CA, USA). The resulting construct was introduced into the modified Rosa26 locus of Balb/c mouse embryonic stem cells by recombinase-mediated cassette exchange as described earlier.[22] Chimeric mice were backcrossed to Balb/c mice and transgenic mice identified by genotyping.[22]

Immunoblotting

Protein lysates were extracted from inguinal mammary glands or tumors using LB buffer (50 mM Tris–HCl pH8, 150 mM NaCl, 1% NP-40) supplemented with 0.5 mM sodium orthovanadate. Anti-p110α, anti-pAKT (Ser473), anti-Akt, anti-pERK1/2 (Thr202/Tyr204), anti-ERK1/2, anti-pS6 (Ser235/236), anti-S6, anti-Akt1, anti-Akt2, anti-pSTAT3 (Tyr705) and anti-STAT3 antibodies were purchased from Cell Signaling Technology, Danvers, MA, USA.

Immunohistochemistry

The following antibodies were used: K14 (Thermo Scientific, , Waltham, MA, USA, RB-9020, 1:100), K18 (Fitzgerald, Acton, MA, USA, #GP11, 1 : 200), ER (Santa Cruz, , Dallas, TX, USA, SC-542, 1:1000), α-SMA (Thermo Scientific, RB-9010, 1:500), cleaved caspase-3 (Cell Signaling, #9661, 1:100) Ki-67 (Thermo Scientific, RB-9106, 1:50).

Southern blotting

Genomic DNA from mouse tails was digested with 8 U of AvrII enzyme (New England BioLabs (NEB), Ipswich, MA, USA) and separated on a 1% agarose gel. A DIG-labeled DNA probe targeting the neomycin resistance cassette was amplified using the PCR DIG Probe Synthesis Kit (Roche, Basel, Switzerland) and the primers 5′-ATGGGATCGGCCATTGAACAAGAT-3′ and 5′-CGGCCATTTTCCACCATGATAT-3′.

CONFLICT OF INTEREST

M Mueller is a Novartis employee. All the other authors declare no conflict of interest.

ACKNOWLEDGEMENTS

We thank members of the Bentires-Alj laboratory for advice and discussions. Research in the laboratory of MB-A is supported by the Novartis Research Foundation, the European Research Council (ERC starting grant 243211-PTPsBDC), the Swiss Cancer League and the Krebsliga Beider Basel.

REFERENCES

1 Yuan TL, Cantley LC. PI3K pathway alterations in cancer: variations on a theme. *Oncogene* 2008; **27**: 5497–5510.
2 Manning BD, Cantley LC. AKT/PKB signaling: navigating downstream. *Cell* 2007; **129**: 1261–1274.
3 Bachman KE, Argani P, Samuels Y, Silliman N, Ptak J, Szabo S *et al.* The PIK3CA gene is mutated with high frequency in human breast cancers. *Cancer Biol Ther* 2004; **3**: 772–775.
4 Kadota M, Sato M, Duncan B, Ooshima A, Yang HH, Diaz-Meyer N *et al.* Identification of novel gene amplifications in breast cancer and coexistence of gene amplification with an activating mutation of PIK3CA. *Cancer Res* 2009; **69**: 7357–7365.
5 Levine DA, Bogomolniy F, Yee CJ, Lash A, Barakat RR, Borgen PI *et al.* Frequent mutation of the PIK3CA gene in ovarian and breast cancers. Clinical cancer research: an official journal of the American Association for Cancer Research 2005; **11**: 2875–2878.
6 Samuels Y, Wang Z, Bardelli A, Silliman N, Ptak J, Szabo S *et al.* High frequency of mutations of the PIK3CA gene in human cancers. Science 2004; **304**: 554.
7 Wu G, Xing M, Mambo E, Huang X, Liu J, Guo Z *et al.* Somatic mutation and gain of copy number of PIK3CA in human breast cancer. *Breast Cancer Res* 2005; **7**: R609–R616.
8 Hafsi S, Pezzino FM, Candido S, Ligresti G, Spandidos DA, Soua Z *et al.* Gene alterations in the PI3K/PTEN/AKT pathway as a mechanism of drug-resistance (review). *Int J Oncol* 2012; **40**: 639–644.
9 Bader AG, Kang S, Zhao L, Vogt PK. Oncogenic PI3K deregulates transcription and translation. *Nat Rev Cancer* 2005; **5**: 921–929.
10 Bader AG, Kang S, Vogt PK. Cancer-specific mutations in PIK3CA are oncogenic in vivo. *Proc Natl Acad Sci USA* 2006; **103**: 1475–1479.
11 Isakoff SJ, Engelman JA, Irie HY, Luo J, Brachmann SM, Pearline RV *et al.* Breast cancer-associated PIK3CA mutations are oncogenic in mammary epithelial cells. *Cancer Res* 2005; **65**: 10992–11000.
12 Zhao JJ, Liu Z, Wang L, Shin E, Loda MF, Roberts TM. The oncogenic properties of mutant p110alpha and p110beta phosphatidylinositol 3-kinases in human mammary epithelial cells. *Proc Natl Acad Sci USA* 2005; **102**: 18443–18448.
13 Koren S, Bentires-Alj M. Mouse models of PIK3CA mutations: one mutation initiates heterogeneous mammary tumors. *FEBS J* 2013; **280**: 2758–2765.
14 Zhao L, Vogt PK. Helical domain and kinase domain mutations in p110alpha of phosphatidylinositol 3-kinase induce gain of function by different mechanisms. *Proc Natl Acad Sci USA* 2008; **105**: 2652–2657.
15 Barbareschi M, Buttitta F, Felicioni L, Cotrupi S, Barassi F, Del Grammastro M *et al.* Different prognostic roles of mutations in the helical and kinase domains of the PIK3CA gene in breast carcinomas. *Clin Cancer Res* 2007; **13**: 6064–6069.
16 Miller TW. Initiating breast cancer by PIK3CA mutation. *Breast Cancer Res* 2012; **14**: 301.
17 Saal LH, Holm K, Maurer M, Memeo L, Su T, Wang X *et al.* PIK3CA mutations correlate with hormone receptors, node metastasis, and ERBB2, and are mutually exclusive with PTEN loss in human breast carcinoma. *Cancer Res* 2005; **65**: 2554–2559.
18 Miron A, Varadi M, Carrasco D, Li H, Luongo L, Kim HJ *et al.* PIK3CA mutations in in situ and invasive breast carcinomas. *Cancer Res* 2010; **70**: 5674–5678.
19 Kalinsky K, Jacks LM, Heguy A, Patil S, Drobnjak M, Bhanot UK *et al.* PIK3CA mutation associates with improved outcome in breast cancer. *Clin Cancer Res* 2009; **15**: 5049–5059.
20 Lai YL, Mau BL, Cheng WH, Chen HM, Chiu HH, Tzen CY. PIK3CA exon 20 mutation is independently associated with a poor prognosis in breast cancer patients. *Ann Surg Oncol* 2008; **15**: 1064–1069.
21 Cancer Genome Atlas Network. Comprehensive molecular portraits of human breast tumours. *Nature* 2012; **490**: 61–70.
22 Meyer DS, Brinkhaus H, Muller U, Muller M, Cardiff RD, Bentires-Alj M. Luminal expression of PIK3CA mutant H1047R in the mammary gland induces heterogeneous tumors. *Cancer Res* 2011; **71**: 4344–4351.
23 Adams JR, Xu K, Liu JC, Agamez NM, Loch AJ, Wong RG *et al.* Cooperation between Pik3ca and p53 mutations in mouse mammary tumor formation. *Cancer Res* 2011; **71**: 2706–2717.
24 Liu P, Cheng H, Santiago S, Raeder M, Zhang F, Isabella A *et al.* Oncogenic PIK3CA-driven mammary tumors frequently recur via PI3K pathway-dependent and PI3K pathway-independent mechanisms. *Nat Med* 2011; **17**: 1116–1120.
25 Tikoo A, Roh V, Montgomery KG, Ivetac I, Waring P, Pelzer R *et al.* Physiological levels of Pik3ca(H1047R) mutation in the mouse mammary gland results in ductal hyperplasia and formation of ERalpha-positive tumors. *PLoS One* 2012; **7**: e36924.
26 Tchorz JS, Kinter J, Muller M, Tornillo L, Heim MH, Bettler B. Notch2 signaling promotes biliary epithelial cell fate specification and tubulogenesis during bile duct development in mice. *Hepatology* 2009; **50**: 871–879.
27 Wintermantel TM, Mayer AK, Schutz G, Greiner EF. Targeting mammary epithelial cells using a bacterial artificial chromosome. *Genesis* 2002; **33**: 125–130.
28 Boulanger CA, Wagner KU, Smith GH. Parity-induced mouse mammary epithelial cells are pluripotent, self-renewing and sensitive to TGF-beta1 expression. *Oncogene* 2005; **24**: 552–560.
29 Booth BW, Boulanger CA, Smith GH. Alveolar progenitor cells develop in mouse mammary glands independent of pregnancy and lactation. *J Cell Physiol* 2007; **212**: 729–736.
30 Bruno RD, Smith GH. Functional characterization of stem cell activity in the mouse mammary gland. *Stem Cell Rev* 2011; **7**: 238–247.